Gold clusters (Au_N, $2 \leq N \leq 10$) and their anions

Hannu Häkkinen and Uzi Landman

School of Physics, Georgia Institute of Technology, Atlanta, Georgia 30332-0430

(Received 10 May 2000)

Atomic and electronic structures of neutral and anionic gold clusters (Au_N and Au_N^-, $2 \leq N \leq 10$) are investigated using the density-functional theory with scalar-relativistic *ab initio* pseudopotentials and a generalized gradient correction. The ground state optimal geometries of the neutral and anionic clusters are found to be planar up to $N=7$ and 6, respectively, with the much studied Au_6^- cluster predicted to have a D_{3h} triangular structure. The calculated electron detachment energies of the ground-state anions exhibit strong odd-even alternations and structural sensitivity and agree quantitatively with photoelectron measurements. Photofragmentation patterns of the cluster anions and their interplay with the photodetachment process, are investigated and correlated with experiments.

Nanoscale gold particles and compounds play an important role in colloidal chemistry,[1] medical science,[2] and catalysis.[3] In light of the above and a recent discovery of extreme size sensitivity of catalytic activity of supported gold clusters[4] (with up to 20 atoms), as well as early observations of reactivity of gas-phase cluster anions,[5,6] there is an urgent need to understand structures and bonding in small neutral and anionic gold clusters.[7]

We report here on systematic density-functional theory (DFT) investigations of the atomic and electronic structures of gold clusters, Au_N, and their anions, Au_N^-, with $2 \leq N \leq 10$. The vertical electron detachment energies (vDE) of the ground-state anions are found to be in very good agreement with photoelectron spectroscopy (PES) data,[8–12] and their structural sensitivity is illustrated through comparison between the values calculated for the ground-state structures and those corresponding to higher-energy isomers. The photofragmentation patterns of the cluster anions exhibit a dependence on cluster size with asymmetric fragmentation favored for all sizes, and the interplay between such processes and electron photodetachment is correlated with results obtained via laser experiments[8] for Au_3^-.

We use the Born-Oppenheimer local-spin-density molecular dynamics (BO-LSD-MD) method,[13] employing scalar-relativistic[14] *ab initio* pseudopotentials for the $5d^{10}6s^1$ valence electrons of gold,[15] and the recent generalized gradient approximation (GGA) by Perdew, Burke, and Ernzerhof (PBE) (Ref. 16) is used for the exchange-correlation potential. For comparison, some calculations for Au_2-Au_4 clusters were repeated without the GGA by using the LSD parametrization by Vosko, Wilk, and Nusair (VWN).[17] All the structures were fully optimized without any symmetry constraints, starting from a large number of initial candidate geometries including the ones discussed in the literature (see, e.g., Refs. 18–20) for group IA (Li,Na,K) and IB (Cu,Ag) clusters in the size range considered in this paper.

The optimized ground state structures of Au_N and Au_N^- clusters, $N=4 \ldots 10$, are shown in Fig. 1. We note that the smallest neutral clusters acquire similar structures as alkali or other IB metals, namely C_{2v} obtuse triangle (obtuse angle of

66.2° and the short bond of 2.63 Å), D_{2h} rhombus, and C_{2v} ''W-shaped'' planar structure for $N=3,4$, and 5, respectively. It is interesting to note that a cluster as large as Au_7 prefers a planar (D_{2h}) structure at variance with alkalis[18] or IB elements Cu (Ref. 19) and Ag.[20] Three-dimensional (3D) structures are preferred for $N \geq 8$: a T_d capped tetrahedron for Au_8, a C_{3v} structure for Au_9, and a C_{2v} structure for Au_{10}.

The anions have 2–4 % expanded bond lengths with respect to the corresponding neutral cluster, and in some cases acquire a different ground state geometry, observed here for $N=3,4,7,8,9$. Au_3^- has a linear structure (bond length of 2.60 Å), Au_4^- has two essentially degenerate structures: one is a C_{2v} ''Y-shaped'' structure, similar to the ground state of
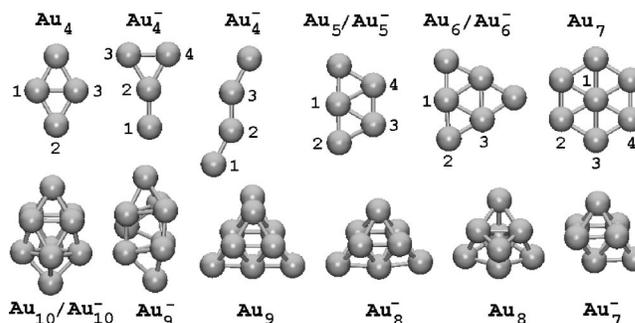

FIG. 1. PBE-GGA optimized structures of neutral and anionic gold clusters with 4–10 atoms; the geometries for the neutrals and anions with $N=2,3$ are given in the text. For Au_4^- we show the two degenerate structures (ys,zz) discussed in the text. For the 2D structures (top row) the pertinent structural parameters for interatomic bond lengths (d_{ij}, in Å) and bond angles (α_{ijk}, in degrees, ijk refer to numbering of the atoms) are as follows: Au_4: $d_{12}=2.70$, $\alpha_{123}=58.9$; Au_4^- (ys): $d_{12}=2.59$, $d_{23}=2.72$, $\alpha_{324}=59.8$; Au_4^- (zz): $d_{12}=2.61$, $d_{23}=2.60$, $\alpha_{123}=152.5$; Au_5: $d_{12}=2.64$, $d_{13}=2.78$, $\alpha_{213}=59.6$, $\alpha_{314}=58.0$; Au_5^-: $d_{12}=2.65$, $d_{13}=2.82$, $\alpha_{213}=60.8$, $\alpha_{314}=56.1$; Au_6: $d_{12}=2.66$, $d_{13}=2.81$; Au_6^-: $d_{12}=2.71$, $d_{13}=2.76$; Au_7: $d_{12}=d_{14}=2.72$, $d_{13}=2.77$. For the 3D clusters (bottom row) the average bond lengths are 2.79, 2.80, 2.80, 2.81, 2.77, 2.81, and 2.82 Å for Au_7, Au_8, Au_8^-, Au_9, Au_9^-, Au_{10}, and Au_{10}^-, respectively. The symmetries of the clusters are discussed in the text.
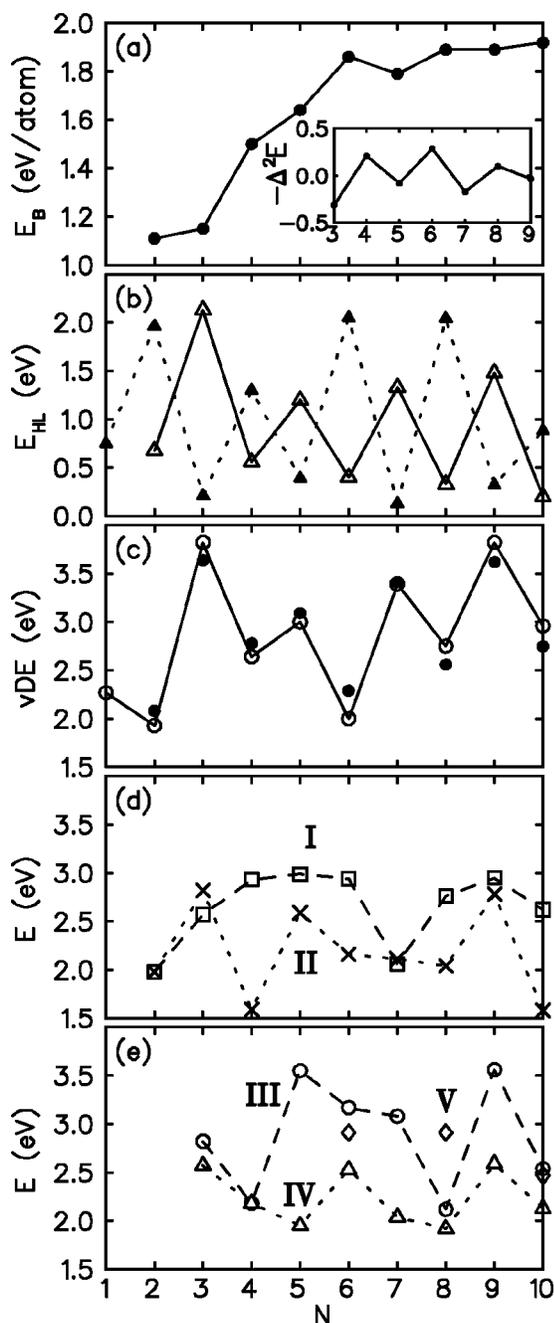
FIG. 2. (a) Binding energy per atom, E_B, for neutral clusters with the inset showing the second difference $-\Delta^2 E$ in the binding energy with respect to the particle number N. (b) HOMO-LUMO gap, E_{HL}, for neutral (solid triangles connected by dashed line) and anionic (open triangles connected by solid line) clusters. (c) Calculated (solid dots) and experimentally measured (Ref. 10, open dots connected by a line) vertical electron detachment energies, vDE. (d),(e) Calculated fragmentation energies for: (d) channels (I) and (II) (open squares and crosses), and (e) channels (III)–(V) (open circles, triangles, and diamonds).

Ag$_4^-$ found in Hartree-Fock–configuration interaction (HF-CI) calculations,[20] and another one is a "zig-zag" structure, not reported previously for any metal cluster anion, to the best of our knowledge. The anions acquire 3D structure for $N \geq 7$: Au$_7^-$ and Au$_8^-$ are C_{3v} and C_{2v} capped and bicapped octahedra, respectively.

In Fig. 2 we display: (a) the calculated per-atom binding

energies $[E_B(N)]$ of the ground state neutral clusters, as well as the second difference in the binding energy (inset), $\Delta^2 E_B(N) = E_B(N+1) - 2E_B(N) + E_B(N-1)$, (b) the HOMO-LUMO energy gaps (E_{HL}), and (c) the vertical detachment energies (vDE) together with the experimental values determined via PES.[10] In general, the PBE-GGA decreases the binding energy by 0.3–0.4 eV per atom compared to the VWN-LSD (e.g., for the dimer the VWN and PBE values are 1.40 and 1.11 eV, respectively) while increasing the interatomic bond lengths by 2–3% (see Fig. 1) (e.g., from 2.48 Å to 2.54 Å for the neutral dimer, and from 2.58 Å to 2.65 Å for the dimer anion). We note that the experimental binding energy of the dimer [1.14 ± 0.05 eV/atom (Ref. 21) and 1.1 eV/atom (Ref. 22)] and the measured bond length [2.47 Å (Ref. 22) are in very good agreement with the calculated PBE-GGA results.

For the neutral clusters both $\Delta^2 E_B(N)$ and E_{HL} exhibit odd-even oscillations, indicating that even-numbered Au$_N$ clusters are relatively more stable than the neighboring odd-numbered sizes. The HOMO-LUMO gap is particularly large for Au$_2$, Au$_6$, and Au$_8$ (1.96 eV, 2.05 eV, and 2.04 eV, respectively). We also note that $E_B(N=6)$ is a local maximum. The anions (at their optimal geometries, which differ from those of the neutral ones for $N=3,4,7,8,9$) show a reverse odd-even oscillation: $E_{HL}(N=odd) > E_{HL}(N=even)$ [see solid line in Fig. 2(b)]. We conclude that the spin-pairing effect stabilizes the clusters (both neutral and anionic) with an even number of electrons.
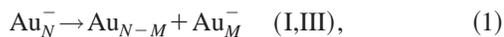
Figure 2(c) shows the calculated energies for vertical detachment of an electron from the ground state cluster anions for $N = 2 - 10$, compared with early PES data.[10] (To the best of our knowledge, up to date this is the most complete single series of measurements in the size range of our interest. Other experimental results,[8,11,12] for a more limited size range of clusters, are in agreement with the data of Ref. 10). The remarkably good agreement between the calculated vDE values and the measured ones (the largest relative deviation, $\sim 15\%$, occurring for Au$_6^-$) validates *a posteriori* our determination of the optimal structures. This is further supported by the often observed sensitivity of the detachment energy (as well as the ionization potential) of small metal clusters to their structure.[20,23] Below, we elaborate on the dependence of the vDE on the isomeric structures of the cluster anions in the case of Au$_4^-$ and Au$_6^-$.

As noted above, Au$_4^-$ has two essentially degenerate structures (see Fig. 1): a C_{2v} "Y-shaped" (ys) structure and a "zig-zag" (zz) structure, as well as two close-lying higher-energy isomers [separated from the nearly degenerate lowest-energy structures by less than 120 K in vibrational temperature T_{vib} (Ref. 24)]: a linear chain (lc) ($D_{\infty h}$) and a rhombus (rh) (D_{2h}); a 3D T_d tetrahedron is a higher-energy, Jahn-Teller unstable, structure. While the linear chain and all the 2D structures described above would be thermally accessible in a typical room-temperature photoelectron experiment,[10] the considerable differences in the vDE values of these structural isomers (2.78 eV, 3.30 eV, 3.53 eV, and 2.64 eV for the ys, zz, lc, and rh structures, respectively) imply that only the ys and rh isomers can contribute to the detachment threshold in the PES spectrum of Au$_4^-$.

Au$_6^-$ has attracted special past interest [9,11,7(a)] due to its exceptionally low vDE of about 2.0 eV, similar to the vDE of Au$_2^-$; these two cluster anions have by far the lowest detachment energies among all the cluster sizes [see Fig. 2(c) and Ref. 10] and PES featuring a large post-threshold gap of 2.5 eV, i.e., the gap between the first (lowest-energy) peak and the next strong feature in the PES (see Fig. 1 of Ref. 9 and Fig. 9 of Ref. 10). This gap would correspond to the HOMO-LUMO gap of the neutral Au$_6$ cluster assuming that the threshold peak of the PES is due to detachment from one electronic state. On the basis of the Hückel model[9] and HF-CI[7(a)] calculations, it had been suggested that the optimal geometry of Au$_6^-$ is a planar D_{6h} ring similar to the carbon ring in a benzene molecule.

Our calculations show that the planar D_{3h} triangular structure (see Fig. 1) is the most stable structure for both Au$_6$ and Au$_6^-$. In this structure, Au$_6^-$ has a low vDE of 2.29 eV (only Au$_2^-$ has a lower calculated vDE), and the corresponding neutral (optimal) cluster has a HOMO-LUMO gap of 2.05 eV [Fig. 2(b)]. Examination of a number of structural isomers for both neutral and anionic Au$_6$ (including D_{5h} capped pentagon, C_{2v} incomplete pentagonal bipyramid, O_h octahedron, $D_{\infty h}$ linear chain, and D_{6h} ring), has verified that: (i) all those anionic isomers lie at least 420 K higher [measured in T_{vib} (Ref. 24)] and they have vDE values ranging from 2.5 to 4.2 eV, and (ii) the HOMO-LUMO gaps of the neutral clusters are less than 1.5 eV. In particular, the D_{6h} ring of Au$_6^-$ is Jahn-Teller unstable (it can be be stabilized against Jahn-Teller deformation only by considering the spin-quartet configuration, i.e., three unpaired electrons, which is, however, 1300 K above the ground state D_{3h} planar structure and has a vDE value of 3.2 eV). We thus conclude that the predicted planar D_{3h} triangular ground state correlates best with both the observed low vDE and the large HOMO-LUMO gap in the neutral cluster.

Upon illuminating metal clusters with a laser, photodetachment of an electron from the cluster and cluster photofragmentation can be competing processes under suitable circumstances, although in general the photodetachment channel is favored over fragmentation if the laser photon energy is high enough (i.e., above the vDE of the cluster anion).[8,25] We have studied the following five channels:

$$\text{Au}_N^- \rightarrow \text{Au}_{N-M} + \text{Au}_M^- \quad \text{(I,III)}, \tag{1}$$

$$\text{Au}_N^- \rightarrow \text{Au}_{N-M}^- + \text{Au}_M \quad \text{(II,IV,V)}, \tag{2}$$

where $M = 1,2$ correspond, respectively, to channels (I) and (III) in Eq. (1), and to channels (II) and (IV) in Eq. (2), and (V) is the symmetric channel with $M = N/2$ for $N = 2,4,6,8,10$. Note that the symmetric channel (V) is degenerate with (I), (II) for Au$_2^-$, and with (III), (IV) for Au$_4^-$. In Figs. 2(d) and 2(e) we show the fragmentation energies for these channels and compare them to the calculated vDE values. Several observations can be made: (i) the energies for electron photodetachment and monomer photofragmentation [channel (II)] are fairly similar for Au$_2^-$ and Au$_6^-$, but differ considerably for all the other sizes (the vDE being higher than the fragmentation energies), (ii) the energetically favored fragmentation channel depends nontrivially on the cluster size, e.g., the optimal channel for Au$_4^-$ and Au$_{10}^-$ is

(II) (losing a neutral atom) while for Au$_5^-$ it is (IV) (losing a neutral dimer), and (iii) the symmetric fragmentation channel (V) is never favored over the asymmetric ones.

Figures 2(d) and 2(e) imply that by lowering the laser energy below the vDE of the cluster in question, photodetachment could be excluded most easily for Au$_N^-$ with $N = 3,5,7,9$, and consequently only fragmentation would be detectable (either by mass spectrometry or through identification of the fragments via analysis of PES data). We note that experiments for Au$_3^-$ corroborate this scenario: In Ref. 8 a photon energy of 3.53 eV (i.e., below the vDE of Au$_3^-$) was used, and the PES of Au$_3^-$ was interpreted as a sum of the spectra of Au$_2^-$ and Au$^-$ associated with a two-photon process (to first fragment the Au$_3^-$ cluster and then to photodetach an electron from the resulting anion). This interpretation is supported by our calculations since both channels (I) and (II) are energetically favored for Au$_3^-$, with their fragmentation energies lying below the vDE of the cluster [compare Fig. 2(d) with 2(c)]. Furthermore, the energetic order of the channels, determined in Ref. 8, agrees with our calculations, namely $E_{frag}(\text{I}) < E_{frag}(\text{II})$.

The results of our study, obtained through state-of-the-art LSD-GGA calculations, give insights into the systematics of the evolution of the geometric and electronic structures of gold clusters (Au$_N$ and Au$_N^-$ with $2 \leqslant N \leqslant 10$). The vDEs of the anionic clusters exhibit a strong structural sensitivity, and the remarkable agreement between the values calculated for the optimal cluster geometries and the measured ones lends further support to our structural assignments. Using these results, as well as the energetics of fragmentation of the anionic clusters, we predict a planar triangular D_{3h} geometry for the much studied Au$_6^-$ cluster, and corroborate the interpretation of laser experiments on Au$_3^-$ cluster involving photofragmentation of the cluster and subsequent electron detachment from the charged fragments.

Finally, we comment that the low vDEs for Au$_{2N}^-$ ($1 \leqslant N \leqslant 5$), associated with large E_{HL} values of the corresponding neutral clusters, with their affinity levels lying above the antibonding (π^*) LUMO of O$_2$, make charge transfer from these clusters to the adsorbed molecule energetically favorable, resulting in weakening of the interoxygen bond and stronger binding to the cluster.[26] This observation correlates with the measured[5] selective reactivity of gas-phase Au$_{2N}^-$ clusters with O$_2$, and with recent[4] experimental and theoretical observations pertaining to the low-temperature catalytic oxidation of CO by Au$_N$ ($8 \leqslant N \leqslant 20$) clusters adsorbed on MgO(001) surfaces. Indeed, for Au$_8$/MgO(001) (with and without surface oxygen vacancies) LSD calculations have shown partial charging of the supported cluster, leading to activation of adsorbed O$_2$, which catalyzes the CO oxidation producing CO$_2$ at temperatures as low as 140 K.[4]

[1] *Colloidal Gold: Principles, Methods, and Applications*, edited by M.A. Hayat (Academic Press, San Diego, 1991).

[2] R.C. Elder *et al.*, J. Am. Chem. Soc. **107**, 5024 (1985), and references therein.

[3] M. Haruta, Catal. Today **36**, 153 (1997).

[4] A. Sanchez, S. Abbet, U. Heiz, W.-D. Schneider, H. Häkkinen, R.N. Barnett, and U. Landman, J. Phys. Chem. A **103**, 9573 (1999).

[5] D.M. Cox *et al.*, Mater. Res. Soc. Symp. Proc. **206**, 43 (1991); Z. Phys. D: At., Mol. Clusters **19**, 353 (1991); T. H. Lee and K. M. Ervin, J. Phys. Chem. **98**, 10 023 (1994); B.E. Salisbury, Ph.D. thesis, Georgia Institute of Technology, 1999.

[6] M.B. Knickelbein, Annu. Rev. Phys. Chem. **50**, 79 (1999).

[7] For previous *ab initio* studies on gold clusters, see, e.g., (a) K. Balasubramanian and D.-W. Liao, J. Chem. Phys. **94**, 5233 (1991), and references therein; (b) O. Häberlen *et al.*, *ibid.* **106**, 5189 (1997); (c) H. Häkkinen *et al.*, Phys. Rev. Lett. **82**, 3264 (1999).

[8] J. Ho *et al.*, J. Chem. Phys. **93**, 6987 (1990).

[9] K.J. Taylor *et al.*, J. Chem. Phys. **93**, 7515 (1990).

[10] K.J. Taylor *et al.*, J. Chem. Phys. **96**, 3319 (1992).

[11] G.F. Gantefor *et al.*, J. Chem. Phys. **96**, 4102 (1992).

[12] H. Handschuh *et al.*, J. Chem. Phys. **100**, 7093 (1994).

[13] R.N. Barnett and U. Landman, Phys. Rev. B **48**, 2081 (1993).

[14] L. Kleinman, Phys. Rev. B **21**, 2630 (1980); G.B. Bachelet and M. Schlüter, *ibid.* **25**, 2103 (1982). The relativistic treatment is crucial for gold as the nonrelativistic pseudopotential would bind the $6s$ electron of the atom much too weakly [we obtained an ionization potential of 7.7 eV and 9.59 eV with nonrelativistic and relativistic potentials, respectively, compared to the experimental value of 9.22 eV (Ref. 21)].

[15] N. Troullier and J.L. Martins, Phys. Rev. B **43**, 1993 (1991). The core radii (in units of a_0) are $s(2.50)$, $p(3.00)$, $d(2.00)$ with s as the local component. See also Ref. 7(c).

[16] J.P. Perdew *et al.*, Phys. Rev. Lett. **77**, 3865 (1996).

[17] S.H. Vosko, L. Wilk, and M. Nusair, Can. J. Phys. **58**, 1200 (1980); S.H. Vosko and L. Wilk, J. Phys. C **15**, 2139 (1982).

[18] U. Röthlisberger and W. Andreoni, J. Chem. Phys. **94**, 8129 (1991).

[19] C. Massobrio *et al.*, J. Chem. Phys. **109**, 6626 (1998).

[20] V. Bonacìc-Koutecký *et al.*, J. Chem. Phys. **98**, 7981 (1993); **100**, 490 (1994).

[21] *CRC Handbook of Chemistry and Physics*, 55th ed., edited by R.C. Weast (CRC Press, Cleveland, Ohio, 1974).

[22] *American Institute of Physics Handbook* (McGraw-Hill, New York, 1972).

[23] J. Akola *et al.*, Phys. Rev. B **60**, R11 297 (1999).

[24] $T_{vib} = 2\Delta E/(3N - 6)k_b$, where N is the number of atoms in the cluster and k_B is the Boltzmann constant.

[25] K. Ervin *et al.*, J. Chem. Phys. **89**, 4514 (1988).

[26] A study of the reactivity of small neutral or anionic gold clusters towards oxygen will be presented elsewhere.